

**Investigating the spatial heterogeneity of factors influencing speeding-related crash severities using correlated random parameter order models with heterogeneity-in-means**

**Renteng Yuan (First author)**

Jiangsu Key Laboratory of Urban ITS  
School of Transportation  
Southeast University, Nanjing, Jiangsu, P. R. China, and 210000  
Email: rtengyuan123@126.com

**Qiaojun Xiang (Corresponding author)**

Jiangsu Key Laboratory of Urban ITS  
School of Transportation  
Southeast University, Nanjing, Jiangsu, P. R. China, and 210000  
Email: 230208815@seu.edu.cn

**Zhiheng Fang**

Jiangsu Key Laboratory of Urban ITS  
School of Transportation  
Southeast University, Nanjing, Jiangsu, P. R. China, and 210000  
Email: 220213476@seu.edu.cn

**Xin Gu**

Beijing Key Laboratory of Traffic Engineering  
Beijing University of Technology, Beijing, P. R. China, and 100124  
Email: guxin@bjut.edu.cn

**Abstract:**

Speeding has been acknowledged as a critical determinant in increasing the risk of crashes and their resulting injury severities. This paper employs Global Moran's I coefficient and local Getis–Ord G\* indexes to systematically account for the spatial distribution feature of speeding-related crashes, study the global spatial pattern of speeding-related crashes, and identify severe crash cluster districts. The findings demonstrate that severe speeding-related crashes within the state of Pennsylvania have a spatial clustering trend, where four crash datasets are extracted from four hotspot districts. Two log-likelihood ratio (LR) tests were conducted to determine whether speeding-related crashes classified by hotspot districts should be modeled separately. The results suggest that separate modeling is necessary. To capture the unobserved heterogeneity, four correlated random parameter order models with heterogeneity in means are employed to explore the factors contributing to crash severity involving at least one vehicle speeding. Overall, the findings exhibit that some indicators are observed to be spatial instability, including hit pedestrian crashes, head-on crashes, speed limits, work zones, light conditions (dark), rural areas, older drivers, running stop signs, and running red lights. Moreover, drunk driving, exceeding the speed limit, and being unbelted present relative spatial stability in four district models. This paper provides insights into preventing speeding-related crashes and potentially facilitating the development of corresponding crash injury mitigation policies.

**Keyword:** Crash severity, Speeding-related crash, Correlated random parameter model, Heterogeneity in means

## 1. Introduction

Speeding behavior has often been regarded as the main primary to crashes and has long been a concern for safety researchers (Aarts & van Schagen, 2006; Ahie et al., 2015; Mohamad et al., 2019; Shyhalla, 2014). In 2020, there were 38,824 fatalities on U.S. roadways, of which, 11,258 (29%) involved at least one vehicle speeding, where speeding-related fatalities accounted for 40.7% of the total (NHTSA). Speeding-related fatalities accounted for 41% (459) of the total 1,129 fatalities in the state of Pennsylvania (NHTSA) in 2020. Therefore, there is an urgent need to develop effective safety strategies to reduce the crash occurrence and minimize crash consequences.

Research has shown that vehicle speed varies in different road segments (Aarts & van Schagen, 2006; Ahie et al., 2015; Mohamad et al., 2019; Wang, X. et al., 2015). Road segments with lower speed limits, central business district areas, secondary roads, lower traffic volume were positively correlated with high rates of speeding (Huang, Y. et al., 2018; Wang, X. et al., 2018). Speeding behavior increases the risk of crashes and affects crash severity (Aarts & van Schagen, 2006). Trends in the clustering of speeding driving behavior may impact the spatial distribution characteristics of speeding-related crashes. Previous studies have confirmed that such clustering area spatial heterogeneity may result in significant variability in the factors affecting crash severity (Song, Li et al., 2020; Wang, C. et al., 2022; Yan et al., 2021). Exploring the spatial distribution pattern of speeding-related crashes is crucial for analyzing crash severity.

A considerable amount of research has been conducted on the macro (zonal) level (e.g., the developing country, the county level, the city level, mountainous areas, rural areas, and work zones) to meet the needs of region-level traffic safety management (Huang, Helai et al., 2010; Lee & Li, 2014; Li, Z. et al., 2013; Rahman et al., 2021; Scheiner & Holz-Rau, 2011; Shafabakhsh et al., 2016; Se, C. et al., 2021, Zeng et al., 2022). Recently, traffic safety analyses at the micro level (e.g., segments, and intersections) have received much attention (Adanu et al., 2021; Chen, Zhang, Liu, et al., 2016; Rezapour & Ksaibati, 2022). At the same time, the limitations of these studies are gradually being reported. For instance, many studies have reported that rural areas increase crash severity and are clusters of severe crashes (Islam, S. & Burton, 2019; Se, C. et al., 2021; Wu et al., 2014). However, some research has also found that not all rural roads are positively associated with an increased likelihood of severe crashes influenced by weather, light conditions, traffic volume, and traffic management measures (Alrejjal et al., 2022; Zhang, K. & M. Hassan, 2019). Therefore, capturing spatial heterogeneity, breaking down the barriers for regional traffic safety analysis (e.g., regional constraints by administrative, urban, and rural areas), and identifying severe crash cluster districts facilitates the accurate prevention and control of traffic accidents. Since previous studies have shown that speeding driving behavior and the injury severity of crashes are, to some extent, induced by factors that change over space, this study is particularly interested in the following problems:

- (1) What is the spatial distribution pattern of speeding-related crashes? How are speeding-related crash hotspot areas identified?
- (2) What are the determinants of speeding-related crash severity? Do significant factors vary across different crash hotspot areas?

The rest of the paper is organized as follows. Section 2 presented a literature review. Section 3 introduces the detailed methodology design. Section 4 introduced the employed dataset. Section 5 conducted two spatial stability tests. Section 6 presented research results and Section 7 summarized the discussions and conclusions.

## **2. Literature review**

An accident will be considered a speeding-related crash if any driver is records as driving too fast for the environment conditions, or exceeding the speed limit of the road (NHTSA; Se et al., 2022). This section summarizes the literature from three aspects: research on speeding-related crash severity, spatial distribution identification methods, and unobserved heterogeneity.

### **2.1 Related work on speeding-related crash severity**

Many studies have been conducted with "speeding driving" as an explanatory variable in the crash severity modeling process (Anarkooli et al., 2017; Rezapour et al., 2019; Se, Chamroeun et al., 2021). These studies concluded that speeding significantly affects crash severity but failed to identify the specific factors affecting the severity of speeding-related crashes. In recent years, very few studies have focused on investigating the factors affecting speeding-related crash severity (Hoye, 2020; Islam, M. & Mannering, 2021; Se et al., 2022). These studies have been fruitful in identifying the significant factors determining speeding-related crash severity. However, no study has been conducted to comprehensively evaluate crash severity considering heterogeneity in the spatial distribution of speeding-related crashes. Ignoring such spatial heterogeneity in speeding-related crash severity analysis may lead to biased results. Therefore, there is a need for a more extensive research on speeding-related crash severity.

### **2.2 Related work on approaches for the spatial distribution of crashes**

Spatial autocorrelation analysis includes both global and local analyses. Before performing local spatial autocorrelation analysis, it is necessary to test the spatial distribution pattern of accidents (global analysis). Nearest neighbor distances, kernel density estimation, and K-function have been developed for the global spatial autocorrelation analysis (Yamada & Thill, 2004), but are limited to equal weights for each point (Songchitruksa & Zeng, 2010). Global Moran's I coefficient, proposed by Griffith (1987), incorporates both the location information and attribute value of points. It has been widely used in global spatial autocorrelation analyses to reflect the spatial distribution pattern of attribute variables (Xiao et al., 2018). For the local spatial autocorrelation analysis (hotspot analysis), the Getis-Ord G\* index and the kernel density estimation (KDE) were employed to identify the "hot" areas of the spatial distribution (Li, Y. et al., 2020; Pulugurtha et al., 2007; Xiao et al., 2018; Alrejjal et al., 2022). Previous studies have indicated that KDE is infeasible for the statistical test (Song, L. et al., 2021; Song, Li et al., 2020). The Getis-Ord G\* index has been widely used to identify locations with spatially aggregated crashes (Pulugurtha et al., 2007; Song, L. et al., 2021; Song, Li et al., 2020), which requires the aggregation of data based on the number of crashes in an area under study divided into smaller space units called rasters (Plug et al., 2011).

### **2.3 Related work on approaches for unobserved heterogeneity**

Many factors significantly affect speeding-related crash severity, such as the driver, vehicle, road infrastructure, and traffic environment. It is unrealistic to consider all factors

when modeling crash severity, which can lead to unobserved heterogeneity (Behnood & Mannering, 2019; Mannering et al., 2016; Wang et al., 2022). The random parameter modeling approach which includes the random parameter ordered probit (RPO-Probit) model, the RPO-Probit model with heterogeneity in means and variance, and the correlated RPO-Probit(CRPO-Probit) model with heterogeneity in means, has been developed to capture unobserved heterogeneity. Previous studies compare the statistical performance of uncorrelated and correlated random-parameter models, reporting that the correlated random-parameter model is statistically superior to uncorrelated models (Saeed et al., 2019; Se, C. et al., 2021; Se, Chamroeun et al., 2021). Therefore, the CRPO-Probit models with heterogeneity in means are conducted in this paper to capture unobserved heterogeneity and provide insights into crash prevention countermeasures.

### 3. Methodology

#### 3.1 Global spatial autocorrelation analysis

Global spatial autocorrelation analysis is mainly focused on identifying the global spatial pattern of space units and investigating their trends. The global spatial pattern contains clustering patterns, discrete patterns and random patterns (Songchitruksa & Zeng, 2010). Local spatial autocorrelation analysis is not required if crashes are randomly distributed in global analysis (Le et al., 2020). In this paper, Global Moran's I coefficient is selected to determine the spatial distribution of speeding-related crashes comes. Global Moran's I is expressed as:

$$I = \frac{\sum_{i=1}^n \sum_{j=1}^n \omega_{ij} (x_i - \bar{x})(x_j - \bar{x})}{\left( \sum_{i=1}^n \sum_{j=1}^n \omega_{ij} \right) \sum_{i=1}^n (x_i - \bar{x})^2} \quad (1)$$

Where  $x_i$  is the attribute value in the  $i$ -th raster (space unit);  $x_j$  is the attribute value in the  $j$ -th raster;  $\bar{x}$  represents the average attribute value in the global space;  $n$  denotes the number of space units of global region,  $\omega_{ij}$  is the spatial weight matrix ( $\omega_{ij} = 1$  if the  $j$ -th raster is in contiguity with the  $i$ -th raster (contiguity edges corners), and 0 otherwise). Global Moran's I coefficient belongs to  $[-1,1]$ , and it will be positive if the pattern of spatial distribution is a clustering pattern (serious crashes tend to cluster in certain districts). Initially, Global Moran's I assumed that the elements in the global space are randomly distributed, and the Z-score of Moran's I is expressed as:

$$Z = \frac{I - E[I]}{\sqrt{V[I]}} \quad (2)$$

Where  $V(I)$  is the variance of Moran's I,  $E(I)$  represents the expectation values of Moran's I and can be calculated as  $E[I] = -1/(n-1)$ . The null hypothesis can be rejected when  $|z| > 1.96$ ,  $p < 0.05$ , (Getis, 2010; Xiao et al., 2018).

#### 3.2 Hotspot Analysis

Hotspot analysis is mainly focused on identifying the severe crash cluster districts, considering the spatial correlation between a raster and its neighboring units. In this paper, the local Getis-Ord  $G^*$  index is selected for local spatial autocorrelation analysis as in previous

studies (Song, Li et al., 2020; Songchitruksa & Zeng, 2010). The local Getis–Ord G\* index is defined as:

$$G_i^* = \frac{\sum_{j=1}^n \omega_{ij} x_j - \bar{x} \sum_{j=1}^n \omega_{ij}}{\sqrt{\frac{\sum_{j=1}^n x_j^2}{n} - \bar{x}^2} \times \sqrt{\left[ n \sum_{j=1}^n \omega_{ij}^2 - \left( \sum_{j=1}^n \omega_{ij} \right)^2 \right] / (n-1)}} \quad (3)$$

Where the local Getis–Ord G\* index is a statistic Z-score, all parameters are explained as described above. For statistically significant positive p-values, a higher score ( $G^* > 0$ ) indicates a tighter clustering of high values (hot spots), a lower  $G^*$  score ( $G^* < 0$ ) denotes a tighter clustering of lower values (cold spots). A statistically insignificant p-value or  $G^* = 0$  means a random pattern of the values.

### 3.3 Correlated random parameter order model with heterogeneity in means

In this research, the CRPO-Probit model with heterogeneity in means is employed. At first, the traditional ordered probit model is defined as follow:

$$y_i^* = \beta_i x_i + \varepsilon_i \quad (4)$$

Where  $x_i$  represents a vector of explanatory variables for the  $i$ -level crash severity,  $\beta_i$  represents a vector of estimable parameters,  $\varepsilon_i$  is random error term and assumed to be normally distributed,  $y_i^*$  is a latent continuous variable that is defined as:

$$y_i = j, \text{ if } u_{j-1} < y_i^* < u_j \quad (5)$$

Where  $y_i$  is the observe injury severity,  $u_j$  represent the threshold parameters,  $j$  is the integers representing the injury-severity levels ( $j = 0, 1, 2$ , respectively, for no injury, minor, and severe injuries). The probability that crash  $i$  being  $j$ -th injury-severity,  $p(y = j)$ , is define as:

$$\begin{aligned} P(y=0) &= \phi(-\beta_i x_i) \\ P(y=1) &= \phi(u_1 - \beta_i x_i) - \phi(-\beta_i x_i) \\ P(y=2) &= 1 - \phi(u_1 - \beta_i x_i) \end{aligned} \quad (6)$$

Where  $\phi$  is the cumulative standard normal distribution. A RPO-Probit model is developed taking into account the effect of unobserved factors. Partial parameters  $\beta_i$  are relaxed and allowed to vary across individual crash observations, as follows:

$$\beta_i = \beta + \zeta_i \quad (7)$$

Where  $\beta$  is the constant term representing the mean value of the random parameters vector,  $\zeta_i$  is the randomly distributed error term (e.g. a normally distributed term with mean=0 and variance  $\sigma^2$ ). Eq. (7) can be extended further by considering interaction effects, as follows:

$$\beta_i = \beta + \eta z_i + \Gamma \omega_i \quad (8)$$

Where  $z_i$  is the vector of independent variables corresponding to random parameters  $\beta_i$ ,  $\eta$  represents a vector of estimable parameters,  $\eta z_i$  is the heterogeneous term to capture

unobserved heterogeneity resulting from interactions between random parameters and fixed parameters (Se, C. et al., 2021),  $\omega_i$  represents a random term with a mean value of zero,  $\Gamma$  is the Cholesky matrix(variance-covariance matrix). The random parameters are assumed to be mutually independent in the RPO-Probit model, and the  $\Gamma$  is defined as a diagonal matrix (Saeed et al., 2019), defined in Eq.(9):

$$\Gamma = \begin{bmatrix} \sigma_{1,1} & \sigma_{1,2} & \cdots & \sigma_{1,n-1} & \sigma_{1,n} \\ \sigma_{2,1} & \sigma_{2,2} & \cdots & \sigma_{2,n-1} & \sigma_{2,n} \\ \vdots & \vdots & \ddots & \vdots & \vdots \\ \sigma_{n-1,1} & \sigma_{n-1,2} & \cdots & \sigma_{n-1,n-1} & \sigma_{n-1,n} \\ \sigma_{n,1} & \sigma_{n,2} & \cdots & \sigma_{n,n-1} & \sigma_{n,n} \end{bmatrix} \quad (9)$$

Where  $n$  represents the number of random parameters,  $\sigma_{k,j}$ ( $1 \leq k \leq n, 1 \leq j \leq n$ ) denotes the elements of the Cholesky matrix. The correlation between random parameters is considered in the CRPO-Probit model, and a generalized Cholesky matrix is defined in Eq.(10),.

$$Var(\beta_i | \omega_i) = \Gamma \Gamma' \quad (10)$$

The diagonal and off-diagonal elements of the  $\Gamma$  matrix are not equal to zero in the generalized Cholesky matrix, and the standard deviations of the correlated random parameters can be computed based on Eq.(11).

$$\sigma_r = \sqrt{\sigma_{k,k}^2 + \sigma_{k,k-1}^2 + \sigma_{k,k-2}^2 + \cdots + \sigma_{k,1}^2} \quad (11)$$

Where  $\sigma_r$  represents the standard deviation of the random parameter  $r$ , and  $\sigma_{k,k}$  is the Cholesky matrix's diagonal element. The correlation coefficient between two random parameters can be determined as:

$$\text{Cor}(x_1, x_2) = \frac{Cov(x_1, x_2)}{\sigma_{x_1} \times \sigma_{x_2}} \quad (12)$$

Where  $\text{Cor}(x_1, x_2)$ represents the correlation coefficient between  $x_1$  and  $x_2$  ,  $\text{Cov}(x_1, x_2)$  denotes the covariance,  $\sigma_{x_1}$  and  $\sigma_{x_2}$  are the standard deviations. In addition, average marginal effects are computed to quantify the effects of category variables on the crash severity, as shown in Eq. (13) (Jalayer et al., 2018).

$$\frac{\Delta P_i(y=j)}{\Delta x} = \left[ \phi(\mu_{j-1} - \beta_i x_i) - \phi(\mu_j - \beta_i x_i) \right] \beta \quad (13)$$

Where  $\phi$  represents the density function of the normal distribution, and all other terms remain defined earlier.

#### 4 Data

The data used in this study were reported by law enforcement agencies from 2018 to 2020 and collected from the Pennsylvania Department of Transportation (PennDOT) Open Data Portal (<https://crashinfo.penndot.gov/PCIT/welcome.html>). For this study, only speeding-related crash records are extracted. Crash identification numbers are employed to link different data files such as crash, vehicle, person, and roadway characteristics. In the connection dataset, one crash record was considered a sample. Ultimately, a total number of 63736 crash records involving speeding was selected. In the original dataset, the injury

severity was coded on the KABCO scale where K-level represented fatal injury, A-level represented suspected serious injury, B-level represented suspected minor injury, C-level represented possible injury, and O-level represented no apparent injury. In this paper, the maximum crash injury level is extracted. The dataset also provides detailed information about the crash location, including latitude, longitude, county, and regional characteristics (urban or rural. The spatial distribution of speeding-related crash data is illustrated in Fig. 1.

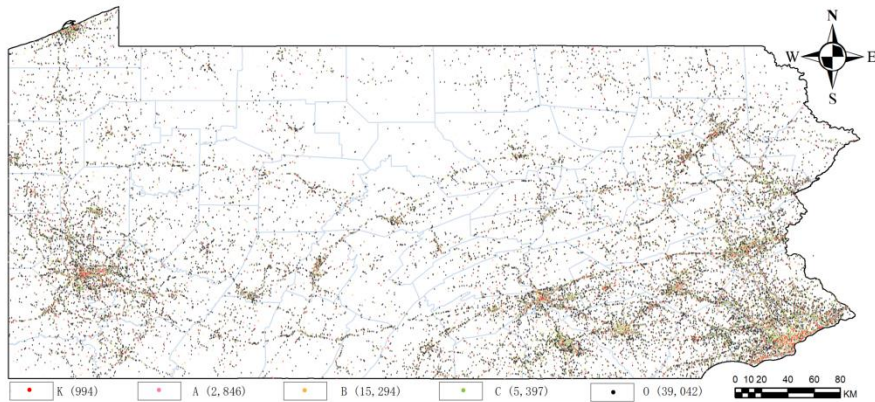


**Fig.1 Spatial distribution of speeding-related crashes**

Note: ( ) is the number of crashes

#### 4.1 Data processing

The state of Pennsylvania is roughly rectangular in shape and stretches about 480 km from east to west and 240 km from north to south. It is further divided into 67,840 rasters (each raster area is about  $1.86 \text{ km}^2$ ) to identify the global spatial pattern of space units. Then, the speeding-related crash data was converted into raster data. Rasters with a speeding-related crash count greater than 0(17,448 rasters) are retained in the dataset, while rasters with crash counts equal to 0 are removed. To accurately describe the casualty level of speeding-related crashes, the equivalent fatalities corresponding to the maximum injury severity are recommended to capture the equivalent impact of an injury relative to a fatality (K-level, A-level, B-level, C-level, and O-level are equivalent to 1, 0.1107, 0.0310, 0.0148, and 0.0049 fatalities, respectively) (Feng et al., 2016).

Global Moran's I coefficient is used to examine the spatial distribution pattern of speeding-related crashes. The corresponding Global Moran's Index is 0.012 (z-score = 9.17, P-value <0.001), indicating a clustering spatial pattern trend within the state of Pennsylvania. Accordingly, hotspot analysis is implemented to identify the district where high and low values of spatial units are clustered. Figure 2 illustrates the result of the Getis-Ord index in the state of Pennsylvania. The red areas represent hotspots, indicating that severe speeding-related crashes tend to cluster in those areas. The blue areas represent coldspots where no injury crashes tend to cluster. Four crash datasets are extracted from four hotspot districts to uncover the causal mechanisms of speeding-related crash severity in hotspot districts, as shown in Fig. 2. The maximum injury severity is aggregated into three injury severity categories: no injury (O-level), minor injury (B-level and C-level), and serious injury (K-level and A-level) in four extracted crash datasets (Islam, S. & Burton, 2019; Lee & Li, 2014). Table1 summarizes the descriptive statistic of the four crash datasets.

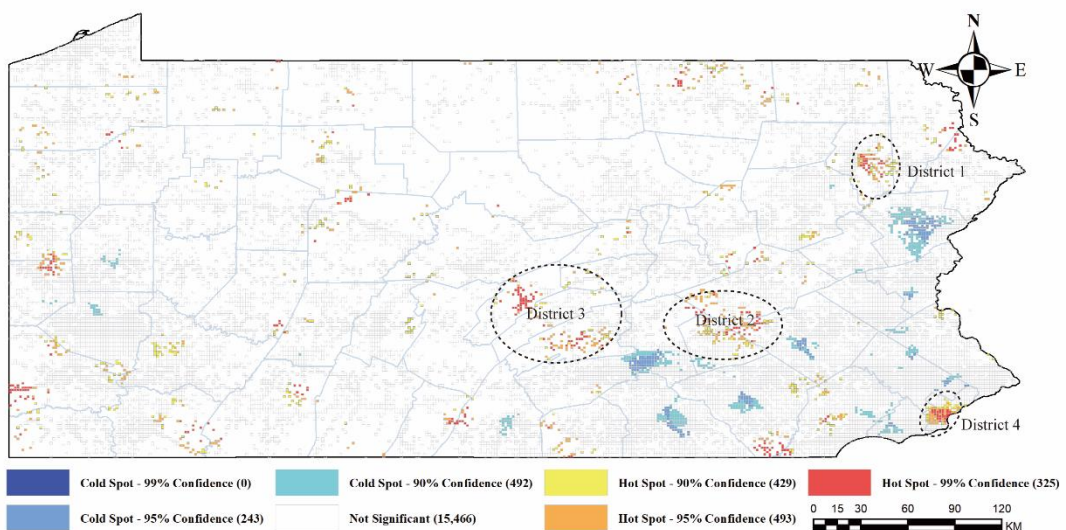


Fig.2. The results of Getis-Ord G\* spatial statistics

Note: ( ) is the number of rasters

**Table 1 Description statistics**

Variables		District 1		District 2		District 3		District 4	
		Means	S.D.	Means	S.D.	Means	S.D.	Means	S.D.
No injury	Total number of the speeding-related crashes with no injury	357		796		447		1613	
Minor injury	Total number of the speeding-related crashes with minor injury	172		367		118		1582	
Serious injury	Total number of the speeding-related crashes with serious injury	47		103		69		238	
<b>Crash Characteristics</b>									
Rear-end	1if the crash was recorded as a rear-end crash, 0 otherwise	.191	.393	.217	.411	.124	.329	.366	.482
Angle crash	1if the crash was recorded as a angle crash, 0 otherwise	.165	.371	.134	.341	.051	.220	.203	.402
Head-on	1if the crash was recorded as a head-on crash, 0 otherwise	.036	.187	.019	.136	.029	.170	.029	.167
Sideswipe	1if the crash was recorded as a sideswipe crash, 0 otherwise	.047	.212	.027	.162	.016	.124	.082	.274
Hit fixed object	1if the crash was recorded as a hit fixed object crash, 0 otherwise	.526	.499	.551	.498	.720	.449	.286	.452
Hit pedestrian	1if the crash was recorded as a hit pedestrian crash, 0 otherwise	.005	.072	.002	.040	.003	.053	.019	.135
Hit bicycle	1if the crash was recorded as a hit bicycle crash, 0 otherwise	0	0	.001	.028	.001	.038	.003	.057
<b>Environment and Roadway characteristics</b>									
State road	1if the crash took place on an state road, 0 otherwise	.233	.423	.188	.390	0	0	.465	.499
Local road	1if the crash took place on a local road, 0 otherwise	.356	.479	.429	.495	.311	.463	.390	.488
Curve road	1if the crash occurred on a curve road segment, 0 otherwise	.330	.471	.359	.480	.474	.499	.175	.380
Speed limit	1 if speed limit $\geq 50$ mile/h , 0 otherwise	.302	.459	.322	.468	.308	.462	.447	.497
Unsignaled intersection	1if the crash took place at an unsignalized intersection, 0 otherwise	.248	.432	.277	.448	.173	.379	.180	.385
Signaled intersection	1if the crash took place at a signaled intersection, 0 otherwise	.125	.327	.085	.278	.031	.174	.235	.424
Snow	1 if the crash involved a snow or slush covered road, 0 otherwise.	.217	.412	.160	.367	.183	.387	.020	.140
Work	1if the crash occurred at work zone, 0 otherwise	.023	.149	.003	.056	.006	.075	.033	.178
Dark	1 if the crashes occurred at night without lights,0 otherwise.	.152	.360	.246	.431	.308	.462	.017	.131

Light	1 if the crashes occurred at night with lights, 0 otherwise.	.222	.416	.08	.272	.048	.211	.439	.496
Rural	1 if crash occurs at rural area, 0 otherwise.	.270	.444	.898	.303	.973	.162	0	0
<b>Driver and vehicle characteristics</b>									
Older driver	1 if the crash involved at least 1 driver age $\geq 60$ , 0 otherwise	.099	.299	.099	.298	.095	.294	.064	.244
Young driver	1 if the crash involved at least 1 driver age $\leq 20$ , 0 otherwise	.179	.384	.238	.426	.288	.453	.141	.348
Drunk driving	1 if the crash involved at least 1 drunk driver, 0 otherwise	.1233	.3293	.055	.227	.079	.270	.050	.217
Exceeding the speed limit	1 if the crash involved at least 1 driver exceeded speed limit, 0 otherwise	.140	.348	.132	.339	.165	.371	.204	.403
Fatigued driving	1 if the crash involved at least 1 driver with fatigued driving, 0 otherwise	.003	.059	.010	.100	.011	.106	.009	.096
Drug related	1 if the crash involved at least 1 driver with drugs reported, 0 otherwise	.057	.232	.025	.157	.041	.199	.027	.163
Running stop sign	1 if the crash involved at least 1 driver ran a stop sign, 0 otherwise	.028	.164	.022	.147	.027	.162	.013	.114
Running red light	1 if the crash involved at least 1 driver ran a red light, 0 otherwise	.014	.117	.012	.112	.006	.075	.020	.140
Unbelted	1 if the crash involved at least 1 person unbelted, 0 otherwise	.135	.342	.103	.305	.136	.343	.148	.355
Large Truck	1 if the crash involved at least 1 truck, 0 otherwise	.073	.260	.137	.344	.061	.239	.053	.225
Overturn	1 if the crash involved at least one overturned vehicle, 0 otherwise	.069	.254	.116	.320	.168	.374	.038	.191

## 5. Spatial Stability Test

Likelihood ratio (LR) test is conducted to determine whether speeding-related crashes classified by severe crash cluster districts should be modeled separately. Firstly, the spatial stability of the parameter estimates between the two districts is tested by Eq. (14)

$$\chi^2 = -2 \left[ \text{LL}(\beta_{m_1, m_2}) - \text{LL}(\beta_{m_1}) \right] \quad (14)$$

Where  $\text{LL}(\beta_{m_1})$  represents the log-likelihood of a converged model using the data collected from district  $m_1$ ,  $\text{LL}(\beta_{m_1, m_2})$  denotes the log-likelihood values of a converged model using both parameters from  $m_2$  and the data from district  $m_1$ , and  $\chi^2$  is a test statistic (chi-square distributed) with degrees of freedom equal to the number of estimated parameters in  $\beta_{m_1, m_2}$  (Behnood & Mannering, 2015). As shown in Tables 2, 9 of all 12 tests produce a confidence level more than 90% (except for  $m_2/m_1$  for District 1/ District 2, District 1/District 3, and District 2/District 3 which produce less than 90% confidence level; however, the reversed tests of these models produce 90% confidence level), indicating that the null hypothesis is rejected at a high confidence level (Yan et al., 2021). Therefore, it can be concluded that the parameters are spatial instability between the two districts.

**Table 2 Likelihood ratio test results between different districts**

m1	m2			
	District 1	District 2	District 3	District 4
District 1	--	17.40(18) [50.4%]	14.88(15) [53.9%]	38.62(17) [99.7%]
District 2	43.92(16) [>99.9%]	--	13.04(15) [40.0%]	47.21(18) [>99.9%]
District 3	24.46(16) [92.1%]	46.34(18) [90.99%]	--	52.64 (18) [>99.9%]
District 4	306.38(16) [>99.9%]	183.72(18) [>99.9%]	106.7(15) [>99.9%]	--

The second likelihood ratio (LR) test is employed between the full model and the four sub-models to further investigate whether speeding-related crashes should be modelled separately at four districts, as shown in Eq. (15).

$$\chi^2_{full} = -2 \left[ \text{LL}(\beta_{full}) - \sum_{\alpha=1}^4 \text{LL}(\beta_{D\alpha}) \right] \quad (15)$$

Where  $\chi^2_{full}$  represents the log-likelihood of a converged model using the speeding-related crash data from four districts,  $\text{LL}(\beta_{D\alpha})$  represents the log-likelihood of a converged model using the crash data from district  $\alpha$ .  $\chi^2_{full}$  follows a chi-square distribution with degrees of freedom equal to the summation of parameters found to be statistically significant in each district minus the number of parameters found to be statistically significant using the data from four districts at the same time. The second LR test result is 234.2 with 25 degrees of freedom suggesting that the null hypothesis can be rejected. Therefore, it can be concluded that speeding related crashes should be modelled separately for four severe crash cluster districts.

## 6 Results

As described in Section 4, the four data subsets are first extracted from hotspot districts. The CRPO-Probit model is used to capture unobserved heterogeneity. All random parameters are assumed to follow a normal distribution, and 1000 Halton draws are employed. Only variables with at least 90% confidence in statistical significance are retained. The parameters' estimate, Akaike information criterion (AIC), t-statistics, goodness-of-fit statistics, likelihood

at convergence, and marginal effect are presented in Table 3.

### **6.1 Crash Characteristics**

Regarding crash characteristics, differences among the significant variables associated with crash severity across the four districts can be observed. Rear-end crashes are significantly positively associated with increased serious injury (by .009) in District 2 but negatively correlated (by .034) in District 3. Sideswipe crashes result in a lower likelihood of serious injury in District 4 (by .012) and present a .017 increase of .017 in District 2. The results further illustrate that the effect of collision characteristics on crash severity is spatial instability.

Rear-end crashes, angle crashes, head-on crashes, and sideswipe crashes are found to increase crash severity in District 2, indicating that more traffic management measures should be implemented in this district that aim to mitigate multi-vehicle (at least two vehicles involved) crash severity. Hit pedestrian crashes are significantly positively associated with increased serious injury (.237), but only in District 4. Therefore, improving pedestrian safety is a priority in District 4. In Districts 1 and 3, crash characteristics are not significantly related to increase crash severity, and more attention should be given to other factors.

### **6.2 Roadway and environment characteristics**

In terms of the roadway characteristics, a speed limit above 50 mi/h in District 4 is associated with a lower probability of serious injury (reduction by .023). The results indicate speeding vehicles on low speed limit road segments in District 4 should receive more attention than those with speed limits above 50 mi/h. Speeding-related crashes at unsignaled intersection increased the probability of serious injury crashes by .0014 in District 1, but heterogeneity was captured in District 2. Signaled intersections are significantly positively associated with increased crash severity in District 4, but negatively associated in Districts 2 and 3. These results suggest that the relationship between crash severity and intersections varies by district. The work zone variable is an influential factor in District 2 and increases the risk of serious injury by .276.

Regarding the environment characteristics, light conditions have been found to play an essential role as a key risk factor influencing speeding-related crash injury severity in Districts 1 and 3. The dark indicator is associated with more severe injuries in District 1. Speeding-related crashes occurring at the night with streetlamps tend to decrease the likelihood of serious injury in Districts 1 and 3. The rural area indicator is significant in District 1, which increases the likelihood of serious injury by .001.

### **6.3 Driver and vehicle characteristics**

Regarding driver characteristics, drivers younger than 20 years of age are associated with serious injuries in District 1 but have random effects in Districts 3 and 4. In District 2, older drivers increase the likelihood of serious- and minor-injury crashes by .008 and 0.157. This result indicates that the age-related indicators vary by district.

The model results also provided evidence of priority districts for traffic enforcement. Driver status during the crash, including drunk driving, speeding (exceeding the speed limit), and not wearing a seatbelt, are significantly positively associated with increased crash severities in the four districts. Fatigued driving increases the likelihood of serious injury crashes by .057 in District 2. Drug-related crashes are found to be significant in Districts 3 and 4. The behavior of running stop signs highly increased crash severity in District 2. Running red lights

increased the possibility of serious injury by .116 in District 1. The model results did not uncover vehicle type differences in crash injury severity. However, overturning increased crash severity in Districts 2, 3, and 4.

#### **6.4 Heterogeneity**

Among the various crash, roadway, environment, driver, and vehicle factors examined, a total of five variables show significant standard deviations, indicating the presence of heterogeneity. For instance, in District 1, a snow or slush road is statistically significant with a mean of -.808 and a standard deviation of .993. The results indicate that a snow- or slush-covered road can reduce the likelihood of serious injury in 65.54% of observations while increasing injury severity in 34.46% of observations. This finding is understandable, as many observed and unobserved factors, such as the road surface type (fresh snow, compacted snow, and slush), snowfall, and traffic volume, have a complex effect on the coefficient of friction (Yasmin, S. & Eluru, 2013). The distribution effect of the random parameters across observations in the four districts is presented in Table 3.

Heterogeneity in the means of random parameters is calculated to further investigate the impacts of the random coefficients. The model results show that intercept is positively associated with unsignaled intersections in District 2, indicating that speeding-related crashes at unsignaled intersections are more dangerous than in other road segments. A curve road increases the mean of speeding driving (exceeding the speed limit) in District 4. This suggests that driving above the speed limit on a curved road increases crash severity.

In addition, correlations between random parameters are also observed in the four districts. Intercepts are positively correlated with the random parameter of “Snow” (.9611) in District 1, indicating that a snow- or slush-covered road is likely to cause severe crash outcomes. In District 2, a negative correlation (-.6127) between intercept and light indicates that speeding-related crashes occurring at night with streetlamps reduce the likelihood of serious injury. Signaled intersection and exceeding the speed limit are found to be negatively correlated with young drivers in District 3 and 4 respectively.

**Table 3 Results of estimated parameters and marginal effects**

Variables	District 1				District 2				District 3				District 4							
	Cor.	t-stat	Marginal effect			Cor.	t-stat	Marginal effect			Cor.	t-stat	Marginal effect			Cor.	t-stat	Marginal effect		
			S	M	N			S	M	N			S	M	N			S	M	N
Constant	-.893	-6.01				-1.058	-12.32				-.131	-1.07				.041	.78			
S.D	1.730	13.57				1.350	18.79													
<b>Crash Characteristics</b>																				
Rear-end						.553	4.78	.009	.187	-.196	-.390	-2.20	-.034	-.099	.134					
Angle crash						.563	4.06	.010	.193	-.204						.192	3.10	.017	.057	-.075
Head-on						1.288	4.38	.071	.410	-.481										
Sideswipe						.670	2.73	.017	.235	-.251						-.163	-2.04	-.012	-.053	.065
Hit fixed object	-1.003	-6.59	-.002	-.308	.311						-.643	-5.12	-.091	-.153	.244	-.339	-6.60	-.025	-.109	.134
Hit pedestrian																1.191	5.67	.237	.127	-.365
<b>Roadway and environment characteristics</b>																				
Speed limit																-.275	-5.28	-.023	-.086	.108
Unsignaled intersection	.541	3.36	.0014	.181	-.182	-.340	-2.80	-.003	-.103	.106										
S.D											1.530	12.94								
Signaled intersection											-.782	-4.10	-.004	-.194	.198	-.459	-1.30	-.036	-.115	.151
S.D															1.045	2.46				
Snow	-.808	-3.04	-.001	-.207	.208	-.523	-3.91	-.003	-.147	.150										
S.D	.993	4.94																		
Work zone								2.133	2.75	.276	.393	-.669								
Dark	.353	1.70	.0008	.117	-.118															
Light	-.352	-1.81	-.0004	-.101	.102										-.409	-1.68	-.034	-.103	.137	
Rural	.437	2.56	.001	.143	-.145															

<b>Driver and vehicle characteristics</b>																				
Older driver					.458	3.25	.008	.157	-.165											
Young driver	.938	5.19	.005	.330	-.335					-.249	-2.18	-.025	-.064	.090	-.085	-1.41	-.006	-.027	.034	
S.D										.270	2.82				.468	7.99				
Drunk driving	.942	4.34	.0058	.337	-.342	1.619	9.60	.116	.463	-.579	.794	4.24	.145	.162	-.308	.386	4.45	.044	.104	-.147
Exceeding the speed limit	1.047	5.37	.0072	.373	-.381	.718	6.02	.016	.247	-.263	.362	2.89	.049	.089	-.138	.282	4.83	.027	.082	-.110
S.D															.606	12.53				
Asleep or Fatigued						1.170	2.95	.057	.384	-.441										
Drug related											.809	3.77	.155	.159	-.314	.236	2.10	.024	.067	-.091
Running stop sign						.538	1.96	.011	.187	-.198										
Running red light	2.173	3.64	.116	.577	-.693															
Unbelted	1.508	7.83	.021	.522	-.543	.896	6.96	.026	.309	-.334	1.090	8.06	.216	.197	-.414	.511	8.88	.058	.135	-.193
Overtake						.780	6.05	.019	.269	-.289	.325	2.63	.043	.081	-.124	.569	5.84	.074	.135	-.209
<b>Heterogeneity in means</b>																				
Constant : Unsigned intersection					.947	3.46														
Exceeding the speed limit:															.337	2.36				
Curve road																				
<b>Threshold parameters</b>																				
$u_1$	2.631	13.33								1.20	14.54				1.873	43.23				
<b>Distribution of random parameters</b>																				

Signaled intersection	33%	67%		
Young driver	17.88%	82..12%	42.86%	57.14%
Exceeding the speed limit			68.08%	31.92%

**Diagonal and off-diagonal matrix[t-stats], and correlation coefficients (in parenthesis) of random parameters**

	<b>District 1</b>		<b>District 2</b>		<b>District 3</b>		<b>District 4</b>
Random parameter	Snow		Light		Signaled intersection		Young driver
Constant	3.456[11.42]( .9611)	Constant	-1.186 [-11.03]( -.6127)	Young driver	-.541[-5.26]( -.565)	Exceeding the speed limit	-.110[-1.91]( -.229)

**Model statistics**

Number of observations		1266		3433	
Number of estimated parameters	16	18	15	18	
LL (0)	Log-Likelihood (only constant)	-496.44	-1082.21	-611.52	-3079.21
LL (β)	Likelihood at convergence	-436.25	-986.15	-536.89	-2780.96
$\rho^2 = 1 - LL(\beta)/LL(0)$		.121	.088	.122	.096
AIC		904.5	2014.3	1103.8	5597.9

**Note :** Variables defined for N = no injury, M= minor injury, N= no injury, Cor.= coefficient, S.D= Standard deviation.

## 7. Discussion

From the crash perspective, the model findings reveal that vehicle-vehicle crashes increase crash severity in District 2, and the head-on collision type tends to be the most dangerous. This finding is logical and consistent with expectations (Hosseinpour et al., 2014; Lee & Li, 2014; Liu, P. & Fan, 2020). Pedestrians are considered the most vulnerable traffic participants (Dai, 2012). Hit pedestrian crash is found to be the most dangerous collision type in District 4. A possible explanation is that pedestrians are directly exposed to crashes (Huang, H. et al., 2008; Li, Yang & Fan, 2018), and speeding vehicles significantly increase pedestrian injury severity. These results indicate that management measures should vary by district. Multi-vehicle crashes (at least two vehicles involved) should be given priority attention in District 2. In contrast, improving pedestrian safety is more important in District 4.

From the roadway perspective, a higher speed limit ( $\geq 50\text{mi/h}$ ) reduces speeding-related crash severity in District 4. This finding contradicts previous studies, which posit that higher speed limits could adversely affect traffic safety (Uddin & Huynh, 2020; Yasmin, S. & Eluru, 2013). Pedestrians feel that crossing when the speed limit is high is more dangerous than in areas with lower speed limits (Demiroz et al., 2015), which may reduce the frequency of illegal road crossing behavior at higher speed limit locations. Speeding at unsignaled and signaled intersections increased crash severity in Districts 1 and 4, respectively, but heterogeneity was captured in Districts 2 and 3. This result is complex and may be caused by the unobserved factors in crash data, such as intersection geometric features, topographical features, and traffic flow characteristics. This finding suggests that the traffic management department should focus on improving the safety of unsignalized intersections in District 1, and on signalized intersections in District 4.

From the environmental perspective, the work zone variable is influential in District 2 but insignificant in other districts. This may be due to the differences in safety regulations at the work zone, as well as the size of the work zone, and the duration of construction (Lym & Chen, 2021). Regarding the effect of lighting conditions, speeding-related crashes occurring at night without streetlamps increase the probabilities of serious injury, while the severity of crashes is reduced in lighted conditions. Poor driver visibility in dark conditions is a major cause of serious crashes (Anarkooli et al., 2017; Jalayer et al., 2018). Drivers are more likely to be faced with unexpected events under dark conditions, and it is difficult for them to identify the risk of a crash quickly. This finding suggests that it is necessary to improve road lighting conditions in District 1. The rural area indicator significantly increases crash severity compared to those that occurred in urban areas in District 1. The higher frequency of vehicle speeding can explain this result due to the lower traffic volume in rural areas.

From the driver and vehicle characteristics perspectives, driver age is a significant factor affecting crash severity. Older drivers are associated with more severe crash outcomes in District 2. Cognitive limitations and physical abilities make older drivers more likely to be involved in serious crashes, especially when faced with speeding-related crashes (Hanrahan et al., 2009; Islam, S. & Burton, 2019). Young drivers are inexperienced but physically strong, leading to the correlation between young drivers and crash severity (especially those related to speeding) varying geographically (Chen, Zhang, Huang, et al., 2016; Lee & Li, 2014). The model results confirmed previous findings that the probability of more severe consequences increases with drunk driving (Adanu et al., 2021; Shyhalla, 2014; Zhang, K. & M. Hassan,

2019), driving exceeding the speed limit (Se, C. et al., 2021; Se, Chamroeun et al., 2021), not wearing a seatbelt (Azimi et al., 2020; Yasmin, S. & Eluru, 2013), and overturning (Peng et al., 2018). At the same time, some driving behaviors are spatially unstable, such as being asleep or fatigued driving, drug-related driving, running stop signs and running red lights. These findings suggest priority areas for traffic enforcement.

## 8. Conclusion and recommendations

The present study focuses on investigating and analyzing variations in the effect of contributing factors on speeding-related crash severity across different severe crash cluster districts. The Global Moran's I coefficient shows a spatial clustering pattern within the state of Pennsylvania. The local Getis-Ord G\* index is then used to identify severe crash cluster districts, and four crash datasets are extracted from four hotspot districts. Two LR tests are conducted to validate whether speeding-related crashes classified by crash cluster districts should be modeled separately. The results suggest that separate modeling is necessary. Four CRPO-Probit models with heterogeneity in means are applied to explore the heterogeneity in crash injury severity outcomes. According to the estimation results, the study provides recommendations to mitigate speeding-related crash severity from the engineering, technology, education, and enforcement perspectives.

From the engineering and technology perspective, improving traffic safety at unsignalized intersections and in dark conditions (without streetlamps) is a priority for District 1. Some traffic management strategies can be considered for implementation, such as improving the visibility of intersections by providing enhanced signing (providing lighting), closing or relocating "High-Risk" intersections, increasing the frequency of road lighting maintenance, and promoting internally illuminated LED traffic sign lights (Shauna Hallmark, 2020). Vehicle-vehicle crashes, work zone, and older drivers significantly contribute to the increased crash severity in District 2. Our study suggests that a unique design consideration is needed for undivided roadways to prevent head-on crashes, where reduced intersection skew angles can be used to prevent angle crashes in District 2. Work zones and special signings, such as those signs used at special events to direct traffic, must be maintained and used correctly. Improving the roadway and driving environment to better accommodate older drivers' unique needs is necessary for District 2. Some measures for improvement include increasing the size and letter height of roadway signs, replacing painted channelization with raised channelization, and implementing wider edge lines (Park et al., 2020). Traffic management in District 4 should give priority to vehicle-pedestrian crashes. Advanced traffic management technology can alleviate this problem by implementing alert system for drivers based on traffic signs, lights, and pedestrian detection.

From the enforcement perspective, this study suggests district priorities for traffic enforcement. For instance, speed enforcement should be prioritized at unsignalized intersections in District 1, while work zones and signalized intersections are paramount in District 2. The traffic management department should focus on the governance of running a red light in District 1. However, prioritizing reducing the running of stop signs and asleep or fatigued driving behaviors would be beneficial for District 2. Our results indicate that drug-related driving is a significant factor in Districts 3 and 4. Therefore, it is necessary to increase the frequency of random law enforcement against drug-related drivers in Districts 3 and 4. Drunk driving and being unbelted are associated with a higher crash severity in all four

districts. Stricter penalties for drunk driving, such as driver's license suspension, increased jail time, and installing an ignition interlock device, could effectively reduce the frequency of drunk-driving. From the education perspective, the traffic management department in District 4 should improve pedestrian safety awareness via more effective ways, such as through awareness campaigns, media. There are also some limitations to be acknowledged in this paper. Firstly, the temporal instability is ignored. Future research may consider spatiotemporal stability in the analysis of speeding-related crash injury severity. Second, CRPO-Probit models ignore the heterogeneity in threshold and variance heterogeneity. Future research may consider relax these restrictions to achieve accurate results.

### **Acknowledgments**

The authors declare that there is no conflict of interest about this manuscript.

### **Reference:**

Aarts, L., & van Schagen, I. (2006). Driving speed and the risk of road crashes: a review. *Accid Anal Prev*, 38(2), 215-224.

Adanu, E. K., Agyemang, W., Islam, R., & Jones, S. (2021). A comprehensive analysis of factors that influence interstate highway crash severity in Alabama. *Journal of Transportation Safety & Security*, 1-25.

Alrejjal, A., Moomen, M., & Ksaibati, K. (2022). Evaluating the effectiveness of law enforcement in reducing truck crashes for a rural mountainous freeway in Wyoming. *Transportation letters*, 14(8), 807-817.

Ahie, L. M., Charlton, S. G., & Starkey, N. J. (2015). The role of preference in speed choice. *Transportation Research Part F: Traffic Psychology and Behaviour*, 30, 66-73.

Alrejjal, A., Moomen, M., & Ksaibati, K. (2022). Evaluating the impact of traffic violations on crash injury severity on Wyoming interstates: An investigation with a random parameters model with heterogeneity in means approach. *Journal of Traffic and Transportation Engineering (English Edition)*.

Anarkooli, A. J., Hosseinpour, M., & Kardar, A. (2017). Investigation of factors affecting the injury severity of single-vehicle rollover crashes: A random-effects generalized ordered probit model. *Accid Anal Prev*, 106, 399-410.

Azimi, G., Rahimi, A., Asgari, H., & Jin, X. (2020). Severity analysis for large truck rollover crashes using a random parameter ordered logit model. *Accident Analysis & Prevention*, 135.

Behnood, A., & Mannering, F. (2019). Time-of-day variations and temporal instability of factors affecting injury severities in large-truck crashes. *Analytic Methods in Accident Research*, 23.

Behnood, A., & Mannering, F. L. (2015). The temporal stability of factors affecting driver-injury severities in single-vehicle crashes: Some empirical evidence. *Analytic Methods in Accident Research*, 8, 7-32.

Chen, C., Zhang, G., Huang, H., Wang, J., & Tarefder, R. A. (2016). Examining driver injury severity outcomes in rural non-interstate roadway crashes using a hierarchical ordered logit model. *Accid Anal Prev*, 96, 79-87.

Chen, C., Zhang, G., Liu, X. C., Ci, Y., Huang, H., Ma, J., . . . Guan, H. (2016). Driver injury severity outcome analysis in rural interstate highway crashes: a two-level Bayesian logistic regression interpretation. *Accid Anal Prev*, 97, 69-78.

Dai, D. (2012). Identifying clusters and risk factors of injuries in pedestrian–vehicle crashes in a GIS

environment. *Journal of Transport Geography*, 24, 206-214.

Demiroz, Y. I., Onelcin, P., & Alver, Y. (2015). Illegal road crossing behavior of pedestrians at overpass locations: Factors affecting gap acceptance, crossing times and overpass use. *Accid Anal Prev*, 80, 220-228.

Feng, S., Li, Z., Ci, Y., & Zhang, G. (2016). Risk factors affecting fatal bus accident severity: Their impact on different types of bus drivers. *Accident Analysis & Prevention*, 86, 29-39.

Getis, A., & Ord, J. K. (2010). The analysis of spatial association by use of distance statistics. In *Perspectives on spatial data analysis* (pp. 127-145). Springer, Berlin, Heidelberg.

Hanrahan, R. B., Layde, P. M., Zhu, S., Guse, C. E., & Hargarten, S. W. (2009). The association of driver age with traffic injury severity in Wisconsin. *Traffic Inj Prev*, 10(4), 361-367.

Hosseinpour, M., Yahaya, A. S., & Sadullah, A. F. (2014). Exploring the effects of roadway characteristics on the frequency and severity of head-on crashes: case studies from Malaysian federal roads. *Accid Anal Prev*, 62, 209-222.

Hoye, A. (2020). Speeding and impaired driving in fatal crashes-Results from in-depth investigations. *Traffic Inj Prev*, 21(7), 425-430.

Huang, H., Abdel-Aty, M. A., & Darwiche, A. L. (2010). County-Level Crash Risk Analysis in Florida: Bayesian Spatial Modeling. *Transportation Research Record: Journal of the Transportation Research Board*, 2148(1), 27-37.

Huang, H., Chin, H. C., & Haque, M. M. (2008). Severity of driver injury and vehicle damage in traffic crashes at intersections: a Bayesian hierarchical analysis. *Accid Anal Prev*, 40(1), 45-54.

Huang, Y., Sun, D. J., & Tang, J. (2018). Taxi driver speeding: Who, when, where and how? A comparative study between Shanghai and New York City. *Traffic Inj Prev*, 19(3), 311-316.

Islam, M., & Manner, F. (2021). The role of gender and temporal instability in driver-injury severities in crashes caused by speeds too fast for conditions. *Accid Anal Prev*, 153, 106039.

Islam, S., & Burton, B. (2019). A comparative injury severity analysis of rural intersection crashes under different lighting conditions in Alabama. *Journal of Transportation Safety & Security*, 12(9), 1106-1127.

Jalayer, M., Shabani, R., Pour-Rouholamin, M., Golshani, N., & Zhou, H. (2018). Wrong-way driving crashes: A random-parameters ordered probit analysis of injury severity. *Accid Anal Prev*, 117, 128-135.

Lee, C., & Li, X. (2014). Analysis of injury severity of drivers involved in single- and two-vehicle crashes on highways in Ontario. *Accid Anal Prev*, 71, 286-295.

Li, Y., Abdel-Aty, M., Yuan, J., Cheng, Z., & Lu, J. (2020). Analyzing traffic violation behavior at urban intersections: A spatio-temporal kernel density estimation approach using automated enforcement system data. *Accid Anal Prev*, 141, 105509.

Li, Y., & Fan, W. (2018). Modelling the severity of pedestrian injury in pedestrian—vehicle crashes in North Carolina: A partial proportional odds logit model approach. *Journal of Transportation Safety & Security*, 12(3), 358-379.

Li, Z., Wang, W., Liu, P., Bigham, J. M., & Ragland, D. R. (2013). Using Geographically Weighted Poisson Regression for county-level crash modeling in California. *Safety Science*, 58, 89-97.

Liu, P., & Fan, W. (2020). Analyzing injury severity of rear-end crashes involving large trucks using a mixed logit model: A case study in North Carolina. *Journal of Transportation Safety & Security*, 14(5), 723-736.

Lym, Y., & Chen, Z. (2021). Influence of built environment on the severity of vehicle crashes caused

by distracted driving: A multi-state comparison. *Accid Anal Prev*, 150, 105920.

Mannering, F. L., Shankar, V., & Bhat, C. R. (2016). Unobserved heterogeneity and the statistical analysis of highway accident data. *Analytic Methods in Accident Research*, 11, 1-16.

Mohamad, F. F., Abdullah, A. S., & Mohamad, J. (2019). Are sociodemographic characteristics and attitude good predictors of speeding behavior among drivers on Malaysia federal roads? *Traffic Inj Prev*, 20(5), 478-483.

NHTSA. United States Department of Transportation. Retrieved from <https://www.nhtsa.gov/risky-driving/speeding>

Park, H. C., Yang, S., Park, P. Y., & Kim, D. K. (2020). Multiple membership multilevel model to estimate intersection crashes. *Accid Anal Prev*, 144, 105589.

Peng, Y., Wang, X., Peng, S., Huang, H., Tian, G., & Jia, H. (2018). Investigation on the injuries of drivers and copilots in rear-end crashes between trucks based on real world accident data in China. *Future Generation Computer Systems*, 86, 1251-1258.

Plug, C., Xia, J. C., & Caulfield, C. (2011). Spatial and temporal visualisation techniques for crash analysis. *Accid Anal Prev*, 43(6), 1937-1946.

Pulugurtha, S. S., Krishnakumar, V. K., & Nambisan, S. S. (2007). New methods to identify and rank high pedestrian crash zones: an illustration. *Accid Anal Prev*, 39(4), 800-811.

Rahman, M. H., Zafri, N. M., Akter, T., & Pervaz, S. (2021). Identification of factors influencing severity of motorcycle crashes in Dhaka, Bangladesh using binary logistic regression model. *Int J Inj Contr Saf Promot*, 28(2), 141-152.

Rezapour, M., & Ksaibati, K. (2022). Contributory factors to the severity of single-vehicle rollover crashes on a mountainous area, generalized additive model. *Int J Inj Contr Saf Promot*, 1-8.

Rezapour, M., Moomen, M., & Ksaibati, K. (2019). Ordered logistic models of influencing factors on crash injury severity of single and multiple-vehicle downgrade crashes: A case study in Wyoming. *J Safety Res*, 68, 107-118.

Saeed, T. U., Hall, T., Baroud, H., & Volovski, M. J. (2019). Analyzing road crash frequencies with uncorrelated and correlated random-parameters count models: An empirical assessment of multilane highways. *Analytic Methods in Accident Research*, 23.

Scheiner, J., & Holz-Rau, C. (2011). A residential location approach to traffic safety: two case studies from Germany. *Accid Anal Prev*, 43(1), 307-322. doi:10.1016/j.aap.2010.08.029

Se, C., Champahom, T., Jomnonkwa, S., Chaimuang, P., & Ratanavaraha, V. (2021). Empirical comparison of the effects of urban and rural crashes on motorcyclist injury severities: A correlated random parameters ordered probit approach with heterogeneity in means. *Accid Anal Prev*, 161, 106352.

Se, C., Champahom, T., Jomnonkwa, S., Karoonsoontawon, A., & Ratanavaraha, V. (2022). Analysis of driver-injury severity: a comparison between speeding and non-speeding driving crash accounting for temporal and unobserved effects. *Int J Inj Contr Saf Promot*, 1-14.

Se, C., Champahom, T., Jomnonkwa, S., Karoonsoontawong, A., & Ratanavaraha, V. (2021). Temporal stability of factors influencing driver-injury severities in single-vehicle crashes: A correlated random parameters with heterogeneity in means and variances approach. *Analytic Methods in Accident Research*, 32

Shafabakhsh, G. A., Famili, A., & Akbari, M. (2016). Spatial analysis of data frequency and severity of rural accidents. *Transportation Letters*, 1-8.

Shauna Hallmark, A. G., Theresa Litteral, Neal Hawkins, Omar Smadi, Skylar Knickerbocker. (2020).

Evaluation of sequential dynamic chevron warning systems on rural two-lane curves. *Transportation Research Record: Journal of the Transportation Research Board*.

Shyhalla, K. (2014). Alcohol involvement and other risky driver behaviors: effects on crash initiation and crash severity. *Traffic Inj Prev*, 15(4), 325-334.

Song, L., Fan, W. D., Li, Y., & Wu, P. (2021). Exploring pedestrian injury severities at pedestrian-vehicle crash hotspots with an annual upward trend: A spatiotemporal analysis with latent class random parameter approach. *J Safety Res*, 76, 184-196.

Song, L., Li, Y., Fan, W., & Wu, P. (2020). Modeling pedestrian-injury severities in pedestrian-vehicle crashes considering spatiotemporal patterns: Insights from different hierarchical Bayesian random-effects models. *Analytic Methods in Accident Research*, 28.

Songchitruksa, P., & Zeng, X. (2010). Getis-Ord Spatial Statistics to Identify Hot Spots by Using Incident Management Data. *Transportation Research Record: Journal of the Transportation Research Board*, 2165(1), 42-51.

Uddin, M., & Huynh, N. (2020). Injury severity analysis of truck-involved crashes under different weather conditions. *Accid Anal Prev*, 141, 105529.

Wang, C., Zhang, P., Chen, F., Cheng, J., & Kim, D.-K. (2022). Modeling Injury Severity for Nighttime and Daytime Crashes by Using Random Parameter Logit Models Accounting for Heterogeneity in Means and Variances. *Journal of Advanced Transportation*, 2022, 1-12.

Wang, X., Fan, T., Chen, M., Deng, B., Wu, B., & Tremont, P. (2015). Safety modeling of urban arterials in Shanghai, China. *Accid Anal Prev*, 83, 57-66.

Wang, X., Zhou, Q., Quddus, M., Fan, T., & Fang, S. (2018). Speed, speed variation and crash relationships for urban arterials. *Accid Anal Prev*, 113, 236-243.

Wu, Q., Chen, F., Zhang, G., Liu, X. C., Wang, H., & Bogus, S. M. (2014). Mixed logit model-based driver injury severity investigations in single- and multi-vehicle crashes on rural two-lane highways. *Accid Anal Prev*, 72, 105-115.

Wang, C., Chen, F., Zhang, Y., & Cheng, J. (2022). Analysis of injury severity in rear-end crashes on an expressway involving different types of vehicles using random-parameters logit models with heterogeneity in means and variances. *Transportation Letters*, 1-12.

Xiao, G., Hu, Y., Li, N., & Yang, D. (2018). Spatial autocorrelation analysis of monitoring data of heavy metals in rice in China. *Food Control*, 89, 32-37.

Yamada, I., & Thill, J.-C. (2004). Comparison of planar and network K-functions in traffic accident analysis. *Journal of Transport Geography*, 12(2), 149-158.

Yan, X., He, J., Zhang, C., Liu, Z., Wang, C., & Qiao, B. (2021). Spatiotemporal instability analysis considering unobserved heterogeneity of crash-injury severities in adverse weather. *Analytic Methods in Accident Research*, 32.

Yasmin, S., & Eluru, N. (2013). Evaluating alternate discrete outcome frameworks for modeling crash injury severity. *Accid Anal Prev*, 59, 506-521.

Zeng, Q., Wang, F., Wang, Q., Pei, X., & Yuan, Q. (2022). Bayesian multivariate spatial modeling for crash frequencies by injury severity at daytime and nighttime in traffic analysis zones. *Transportation Letters*, 1-8